Summary: Two well-characterized metallocene isotactic poly(propylene) (iPP) samples, one of high and one of low molecular weight, were blended together for studying the effects of a second component on quiescent and shear-induced crystallization. A small amount of added high molecular weight (HMW) (up to 10 wt.-%) polymer increases the quiescent crystallization rate. This was observed as a decrease in characteristic halftime of transmitted light intensity. The crystallization halftime increases again when adding more than 10 wt.-% of HMW polymer. The crystallization halftime of pre-sheared samples decreases with increasing HMW fraction and is lowest for the HMW sample by itself. For the specific shearing conditions ($\gamma = 600$, $T_x = 145\,^{\circ}C$), wide-angle X-ray diffraction (WAXD) images show the presence of the gamma (γ) crystalline phase of iPP for samples containing 25 wt.-% of HMW and higher. DSC thermograms demonstrated higher crystalline fractions with increasing HMW fraction in pre-sheared samples.

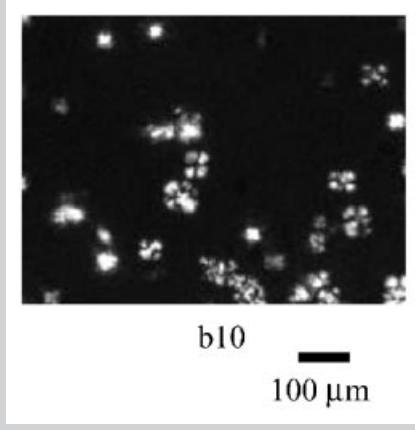

Optical micrograph of an iPP sample after quiescent crystallization at 145 °C.

Isotactic Poly(propylene) Crystallization: Role of Small Fractions of High or Low Molecular Weight Polymer

Aadil Elmoumni,[1] *Ramon A. Gonzalez-Ruiz,*[2] *E. Bryan Coughlin,*[2] *H. Henning Winter**[1,2]

[1] Department of Chemical Engineering, University of Massachusetts Amherst, 159 Goessmann Lab, Amherst, MA 01003, USA
Fax: +1 413-545-1647; E-mail: winter@ecs.umass.edu
[2] Department of Polymer Science and Engineering, University of Massachusetts Amherst, Conte Research Center, 120 Governors Drive, Amherst, MA 01003, USA

Received: April 1, 2004; Revised: July 28, 2004; Accepted: July 30, 2004; DOI: 10.1002/macp.200400130

Keywords: blends; crystallization; isotactic poly(propylene) (iPP); shear

Introduction

A high molecular weight component in a polymer has long been assumed to increase the crystallization rate in sheared or stretched samples.[1–6] In his pioneering work, Pennings et al.[1,7,8] observed shish-kebab structures during crystal formation from polymer solutions under the influence of extensional flow. This was explained by the coexistence of both highly stretched and essentially unstretched chains. The stretched chains crystallize first, giving rise to aligned molecular assemblies on which unstretched chains can nucleate and grow into larger crystals of chain-folded lamellae, usually on subsequent cooling of the system. The long molecules are assumed to stretch the most in a broad molecular weight distributed polymer sample with the shorter molecules remaining less extended. Shish-kebab formation was seen to be highly fractionating, the fiber portion precipitating first and containing the longest molecules. Similar observations of the shish-kebab structure were reported in shear flow.[2,4,6]

During the early part of crystallization, the polymer is far away from equilibrium. Most influential is the molecular orientation of the polymer melt when crystallization begins, i.e. the initial condition for the nucleation and growth process. Experimentally, Janeschitz-Kriegl et al. introduced a short time shearing protocol to modify this initial molecular conformation of the polymer melt.[9–11] The polymer is deformed as soon as the crystallization temperature is reached and subsequent isothermal crystallization is monitored. This protocol has the advantage that it combines high stress, characteristic of processing, with well-defined thermal and flow conditions (isothermal crystallization following a brief interval of shear). The protocol separates the effects of flow from thermal transients or temperature

 DOI: 10.1002/macp.200400130

gradients. Parameters were shear rate or shear stress and their duration. Several research groups have adopted this approach for their experimental work.[12,13]

High molecular weight fractions have been reported to have a large effect on shear-induced crystallization of a polymer. For a blend of two broad molecular weight distribution commercial poly(propylene)s (PP), Nogales et al.[5] reported that only polymer chains above a ''critical orientation molecular weight'' (M^*) can become sufficiently oriented at a given shear rate. Seki et al.[6] demonstrated that a small amount of large chains (high molecular weight tail) boosts the formation of oriented precursors and profoundly affects the crystallization kinetics and crystalline morphology of a sheared melt. Small traces of HMW component already result in a pronounced effect. Seki further enhanced the crystallization rate by choosing a Ziegler-Natta PP of much higher melting temperature, about 15 K degrees higher for the HMW fraction than the metallocene low molecular weight PP.

A commonly used parameter for quantifying the effect of flow is the Weissenberg number (*We*), the dimensionless product of a characteristic relaxation time and the shear rate. Elmoumni[14] and Acierno[15] have recently used *We* to scale the spherulite to shish-kebab structure transition. It was shown that, when using the inverse frequency of the crossover of G' and G'' as characteristic relaxation time, the transition occurs at about $We = 1$. The applied total shear strain was 600. Further studies of the strain effect are in progress. Similar observations were reported by Xu et al.[16] on poly(vinylidene fluoride) using the Deborah number.

The present work focuses on the effect of a second component on the crystallization of iPP. Small amounts of HMW to LMW were added and, vice versa, small amounts of LMW into HMW iPP. Specifically, narrow molecular weight distributions for the two polymers were chosen, and equal molecular compositions and tacticity. While all crystallization occurred without flow, in one group of experiments the samples were crystallized after having been equilibrated in the melt state (''quiescent'' samples) while in a second set of experiments polymers were subjected to a deformation history prior to their crystallization (''presheared'' samples).

Experimental Part

Synthesis and Characterization

Two highly isotactic PPs were produced through solution polymerization in toluene, using *rac*-Si$(CH_3)_2$-(2-CH_3,4-C_6H_5-indenyl)$_2ZrCl_2$ (**I**) (Boulder Scientific Co., Mead, CO) activated with a 30 wt.-% Methylaluminoxane (MAO) in toluene solution (Albemarle Corp., Baton Rouge, LA) as catalytic species. A semi-batch reaction system was used for the controlled production of both PPs, and its details are described elsewhere.[17] Specific reaction conditions for both experiments were 200 ml of dry toluene as solvent, 1 000 rpm of agitation speed, and a MAO/Zr molar ratio of 2 000. The HMW sample (iPP302, $\overline{M}_w = 302\ kg \cdot mol^{-1}$) was produced at a propylene partial pressure of 43 psig, a reactor temperature of 45 °C, employing 0.3 μmol of **I**. The LMW material (iPP140, $\overline{M}_w = 140\ kg \cdot mol^{-1}$) was produced at a propylene partial pressure of 29 psig, a reactor temperature of 55 °C, employing 0.6 μmol of **I**. After a reaction time of 20 min, the reaction was stopped by injection of methanol for both preparations. The propylene atmosphere was replaced by an inert gas and, after venting the vessel, the polymer slurry was washed with acidified methanol and filtered. The solid was dried under vacuum until constant weight.

Gel Permeation Chromatography (GPC) was performed on a Polymer Laboratories PL-220 high temperature GPC instrument at 135 °C, using a Wyatt high-temperature miniDAWN light scattering detector with a 690 nm diode laser; a d*n*/d*c* value of −0.105 was used for the light scattering detector and 1,2,4-trichlorobenzene (TCB) served as solvent (Figure 1). Isotactic poly(propylene) is known as a very difficult material to dissolve, because of its tendency to form stable aggregates, even at high temperatures. To overcome this problem during sample preparation before GPC, it was necessary first to dissolve iPP in decahydronaphthalene (decalin) at a temperature between 120–150 °C for several hours (as decalin increases iPP solubility),[18] and then precipitate the solution in methanol or acetone. The resulting solidified material was then dissolved in TCB at 135 °C and this solution was used for GPC testing. If the polymer samples are dissolved only in TCB before GPC characterization, solubility problems impacting the determination of the molecular weight distribution were observed. Melting points were determined by DSC (TA Instruments 2910), using a heating rate of $10\ K \cdot min^{-1}$ and a continuous nitrogen purge rate of $50\ ml \cdot min^{-1}$. Results listed (see Table 1) are from the second heating scan. High temperature ^{13}C NMR spectra were performed at 100 °C using a Bruker AVANCE D600 FT NMR spectrometer at 150 MHz and 1,1,2,2-tetrachloroethane-d_2 as solvent on selected samples to determine isotacticity at the pentad level.

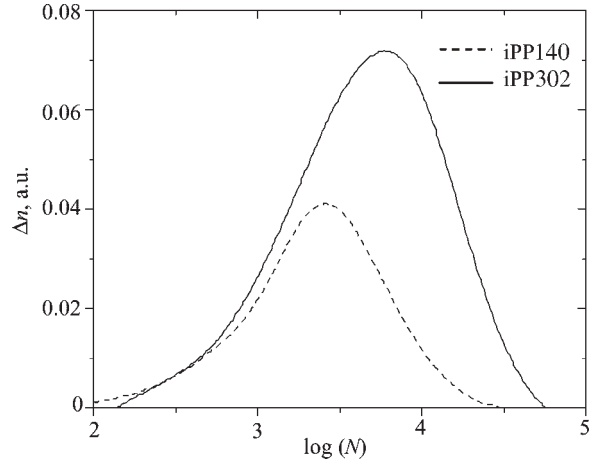

Figure 1. High temperature GPC data of the two iPP samples at 135 °C in 1,2,4-trichlorobenzene.

Table 1. Characteristics of samples utilized to study the effects of long chains on the crystallization of iPP.

Sample	$\bar{M}_w$	$\bar{M}_n$	$\bar{M}_w/\bar{M}_n$	T_m	[*mmmm*]
	$kg \cdot mol^{-1}$	$kg \cdot mol^{-1}$		°C	mol-%
iPP140	140	53	2.67	156.5	96.6
iPP302	302	97	3.11	157.8	96.3

Mixing Procedure and Sample Preparation

In order to prepare homogenous mixtures of the two homopolymers, the various mixtures were ground and weighted at the desired content of HMW (HMW fraction varied between 0.5 to 75 wt.-%, mixtures were labeled bX, where X is high molecular weight fraction in weight percent) and subsequently dissolved in 100 ml of TCB at 130 °C for 30 min in the presence of 2 000 ppm of antioxidant (IRGANOX1010, Ciba Specialty Chemicals). Both homopolymers were also subjected to the same mixing procedure to ensure the same history for all samples. The solution was then quickly poured into 500 ml of methanol, causing aggregation and precipitation. The liquid phase, TCB-Methanol, was separated from the polymer through decantation, and remaining solid material was washed with fresh methanol several times. The wet material was dried under vacuum at 70 °C for 12 h, and a new round of methanol washes were performed if the odor of TCB was still evident. More antioxidant was added, through solid mixing, to the blends before molding at 200 °C for 15 min into 12 mm diameter disks of 1 mm thickness.

Rheological and Optical Tests

Melt rheometry experiments were performed in a rotational rheometer (Stresstech, ATS RheoSystems) equipped with cone-plate fixtures (diameter 25 mm, 4° angle). Sample disks were melted directly in the rheometer for melt rheology studies. Frequency sweeps, in a frequency range of 0.1 to 100 $rad \cdot s^{-1}$, were performed at temperatures from 220 to 140 °C.

For the optical studies, a shearing hot-stage (CSS 450 of Linkam Scientific Instruments) suitable for both microscope and transmittance setup held the sample between concentric discs in a gap of about 200 μm. The shear rate varies radially but is approximately constant along the light path, which is directed normal to the disk. A shear rate $\dot{\gamma} = 10\ s^{-1}$ was selected (at the radial position of the window of the Linkam device) for a duration of 60 s.

Each crystallization experiment began by mounting the polymer sample into the Linkam hot-stage and heating to 200 °C for 15 min to erase effects of previous thermal and mechanical histories. The sample was cooled to the experimental temperature, $T_x = 145$ °C (below T_m) (see Figure 2), and held there for isothermal crystallization. The structure growth was monitored with optical microscopy (OM) and transmitted intensity measurements (TI). For shear-induced crystallization, the actual shear flow was started as soon as the experimental temperature of 145 °C was reached.

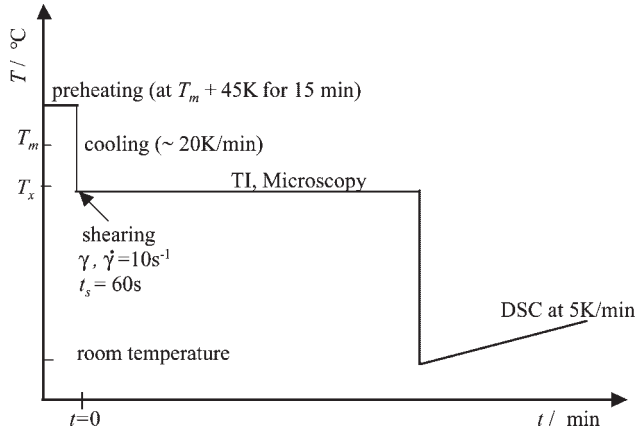

Figure 2. Temperature and shearing protocol applied for crystallization study.

Growing structures were observed under a Universal Polarizing Microscope (Carl Zeiss, model ZPU01). Transmitted intensity was measured in a self-built rheo-optical setup.[4] Light from a 10 mW He-Ne laser (wavelength of 632.8 nm) passed through the sample and was analyzed using a polarizing beam splitter with its axis at −45° to the flow direction. Two detectors measure the intensity of light through crossed and parallel polarizers. The sum of these two intensities represents the total light transmitted through the sample. The total intensity, normalized by the intensity of light transmitted initially through the molten sample, decreased as crystallites form and scatter light. This provided an excellent tool to follow rapid crystallization kinetics. In order to quantitatively describe the crystallization kinetics a turbidity half time, $\tau_{1/2}$, is introduced. It is defined as the time where the normalized transmitted light intensity has decayed to half its initial value.

The final iPP crystal structure, after crystallization, was evaluated with WAXD using a flat plate Statton camera with Ni-filtered Cu-K_α radiation. Melting endotherms were measured by heating from room temperature to 200 °C at a rate of $5\ K \cdot min^{-1}$ in a differential scanning calorimeter (Q1000 of TA Instruments). For comparison, samples were also melted directly after having been crystallized (at temperature $T_x = 145$ °C) without any in-between quench to room temperature.

Results

Melt rheology was carried out on the polymers to study their flow behavior, while in situ rheo-optical measurements along with optical microscopy monitored structural changes during crystallization. WAXD and DSC analyzed the resulting crystalline fractions.

Rheology

Dynamic mechanical data of iPP strongly depend on temperature; see Figure 3 for blend b25. Time-temperature superposition (by simultaneous horizontal and vertical shifting) yields master curves at the reference temperature

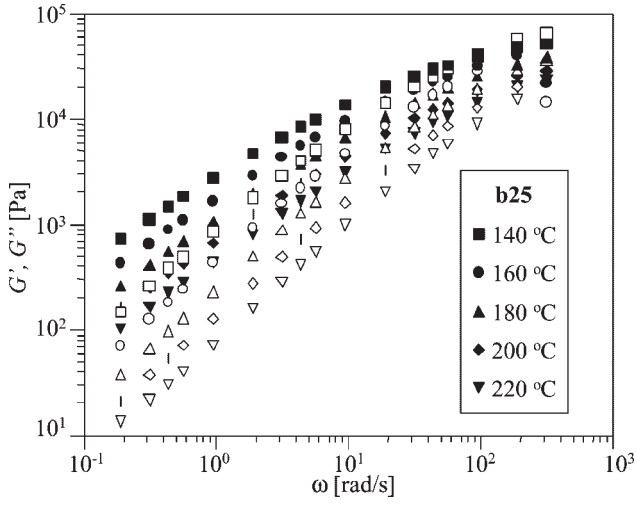

Figure 3. Storage modulus G' (hollow symbols) and G'' (full symbols) of blend b25 obtained from frequency sweeps at temperatures between 140 and 220 °C.

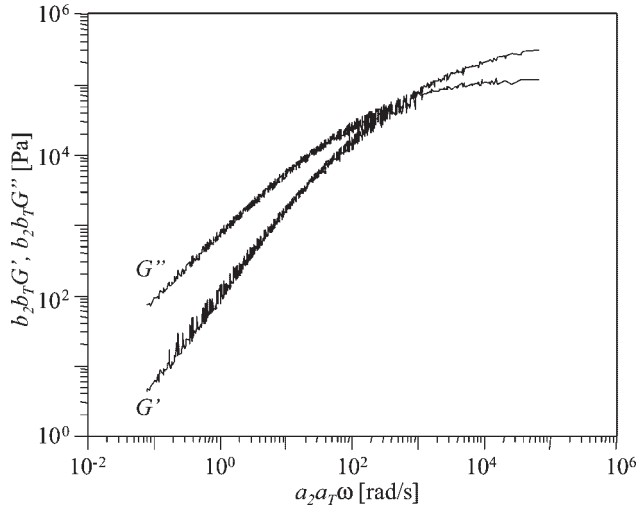

Figure 5. Storage and loss moduli G' and G'' at 145 °C shifted onto iPP140. The master-curves of Figure 4 were further shifted by time-concentration superposition. Time-concentration shifting applies only approximately as shown by the scatter in the "master-curve".

$T_{ref} = 145$ °C that was chosen as the experimental crystallization temperature for both homopolymers and for their blends (see Figure 4). All iPP samples exhibit the typical linear viscoelastic behavior of a highly entangled polymer melt. The crossover of G' and G'' occurs at lower and lower frequencies as the high molecular weight fraction in the blends increases.

All master-curves (after time-temperature superposition) have about the same shape. We make use of this property in a second shifting process. For this "time-concentration shift", the low molecular weight iPP140 was chosen as reference. All data fall into a single master-curve in reasonable approximation (see Figure 5). The corresponding concentration (or molecular weight fraction) shift factors a_2 and b_2 are shown in Figure 6. The purpose of this shifting is to generate relative time constants for all samples:

$$\frac{\lambda_{\text{sample}}}{\lambda_{\text{iPP140}}} = a_2 \tag{1}$$

$\lambda_{\text{iPP302}}/\lambda_{\text{iPP140}}$ is about 233 (see Table 2).

Transmittance

When crystallizing without flow, the time evolution of the total transmitted intensity strongly depends on the concentration of high molecular weight polymer, see Figure 7a and 7b. At the chosen crystallization temperature of $T_x = 145$ °C, the intensity remains almost constant for times up to

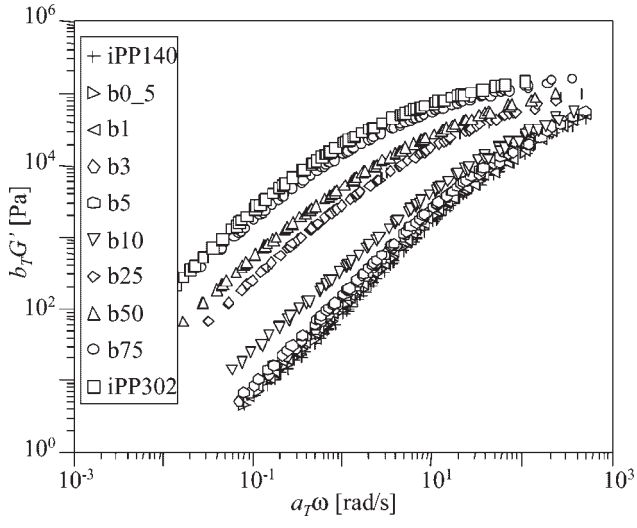

Figure 4. Storage modulus G' of two homopolymers and their blends shifted to master-curves at 145 °C.

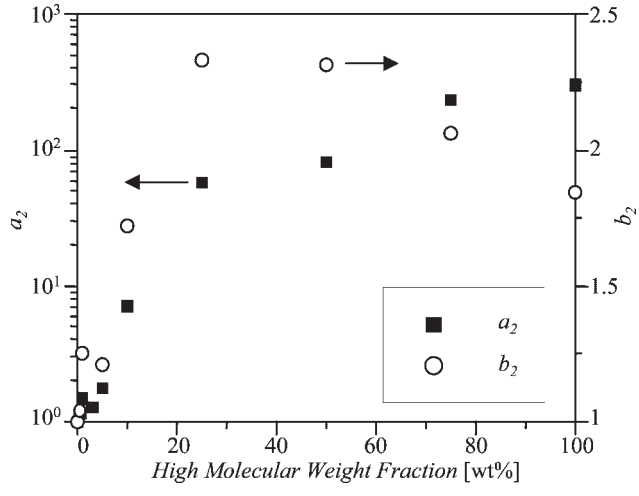

Figure 6. Horizontal and vertical shift factors (time-concentration-shift) as function of high molecular weight fraction at 145 °C.

Table 2. Blends compositions and their characteristic relaxation times from rheological measurements (shifted to 145 °C). Last column shows computed Weissenberg number by multiplying relaxation times λ_i by shear rate used $\dot{\gamma} = 10\ s^{-1}$.

Sample	LMW	HMW	λ_i	$We = \dot{\gamma}\ \lambda_i$
	wt.-%	wt.-%	s	
iPP140	100	0	2.86×10^{-3}	2.86×10^{-2}
b0.5	99.5	0.5	3.33×10^{-3}	3.33×10^{-2}
b1	99	1	4.76×10^{-3}	4.76×10^{-2}
b3	97	3	5.00×10^{-3}	5.00×10^{-2}
b5	95	5	5.40×10^{-3}	5.40×10^{-2}
b10	90	10	1.25×10^{-2}	1.25×10^{-1}
b25	75	25	9.10×10^{-2}	9.10×10^{-1}
b50	50	50	1.25×10^{-1}	1.25
b75	25	75	3.87×10^{-1}	3.87
iPP302	0	100	6.66×10^{-1}	6.66

about 10^4 s. During this initial period, the polymer remains in a state of undercooled melt until nuclei have formed. The subsequent growth of crystallites is observed as a reduction of transmitted light intensity. It decays to nearly zero when the crystallite structures (spherulites under quiescent conditions) grow large enough to touch each other. The sample then becomes fully turbid and reflects almost all of the laser light.

The crystallization process of iPP140 is accelerated by the addition of small amounts of iPP302 (Figure 7a). However, this effect is reversed if the iPP302 fraction gets too large (above 10 wt.-%, see Figure 7a). The turbidity half time as a function of high molecular weight fraction (Figure 8) shows this atypical behavior in quiescent crystallization. The quiescent crystallization rate (expressed by $\tau_{1/2}$) is about the same for pure iPP140 and iPP302. The addition of small amounts of a second component (shorter molecules in a mainly high molecular weight iPP or vice versa) reduces $\tau_{1/2}$, i.e. it increases the crystallization rate. The effect is more pronounced when adding HMW to LMW than when adding LMW to HMW (see Figure 8). $\tau_{1/2}$ is reduced to about 1/4 of its value (of pure iPP140) when adding 10% of iPP302.

After application of shear, the crystallization kinetics changes dramatically compared to quiescent conditions. Figure 9 shows the evolution of the normalized transmitted light intensity of all polymer samples after application of a shear strain $\gamma = 600$ (shear rate $\dot{\gamma} = 10\ s^{-1}$, $t_s = 60$ s). Pure iPP302 shows faster crystallization kinetics compared to pure iPP140. This behavior is attributed to the extension of long chains in the HMW polymer to form row nuclei that lead to the growth of shish-kebab structures as discussed in the morphology section below. $\tau_{1/2}$ in the case of shear flow decreases with increasing high molecular weight fraction (see Figure 10). The lowest value is found with the HMW iPP by itself.

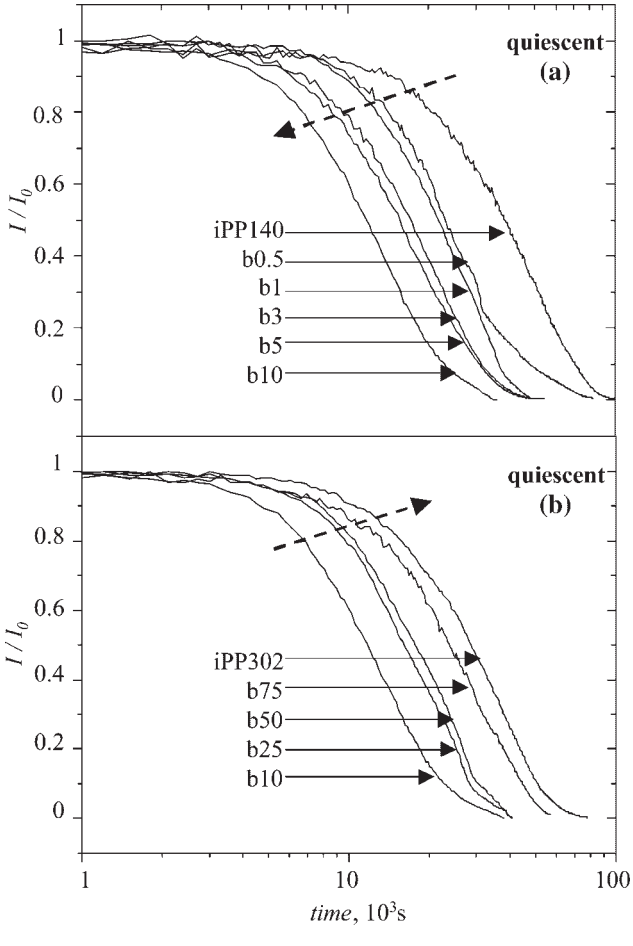

Figure 7. Crystallization without flow. Evolution of normalized transmitted light intensity after quenching of equilibrated samples to 145 °C. Parameter: increasing high molecular weight fraction (as symbolized by dashed arrow direction). Top (a): low concentration; bottom (b): high concentration of HMW.

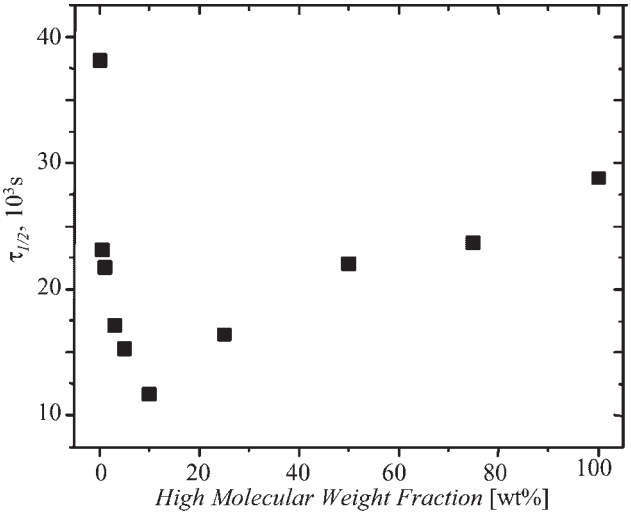

Figure 8. Crystallization without flow. Characteristic crystallization half times at 145 °C with increasing high molecular weight fraction.

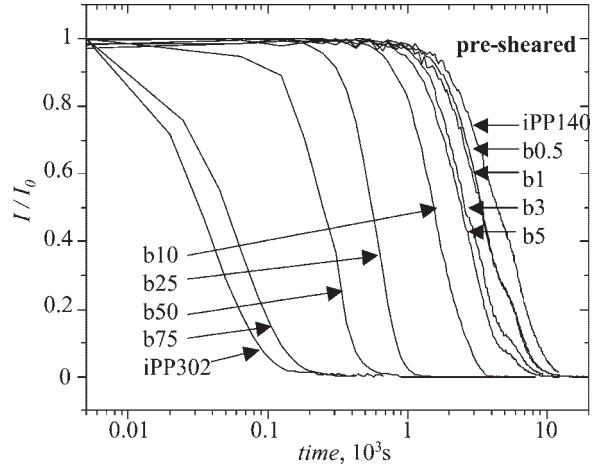

Figure 9. Crystallization of pre-sheared samples with increasing high molecular weight fraction. Evolution of normalized transmitted light intensity at 145 °C.

Morphology

Optical microscopy of selected samples at increasing HMW fraction is shown in Figure 11 and 12. The samples crystallized under the same conditions as for the light intensity studies. In quiescent crystallization (Figure 11), only a few nuclei appear in the beginning and their number stays constant from thereon; blend b10 grows the most spherulites of all samples, including both homopolymers, which may explain the fast kinetics in transmitted light intensity measurements (see Figure 11). Since all observed spherulites grow at the same rate and their observed size is uniform suggests that the nuclei are formed immediately after cooling to the crystallization temperature and their number stays constant thereafter. The nucleus density increases for all samples as shear flow is applied prior to the isothermal crystallization (see Figure 12).

For the chosen experimental conditions, blends with 25% or higher HMW fractions are the only ones to develop shish-kebab structure. The aligning of the shish-kebab structure in the flow direction is visible starting from the early stages of crystallization. This transition from spherulitic to shish-kebab morphology is correlated with the Weissenberg

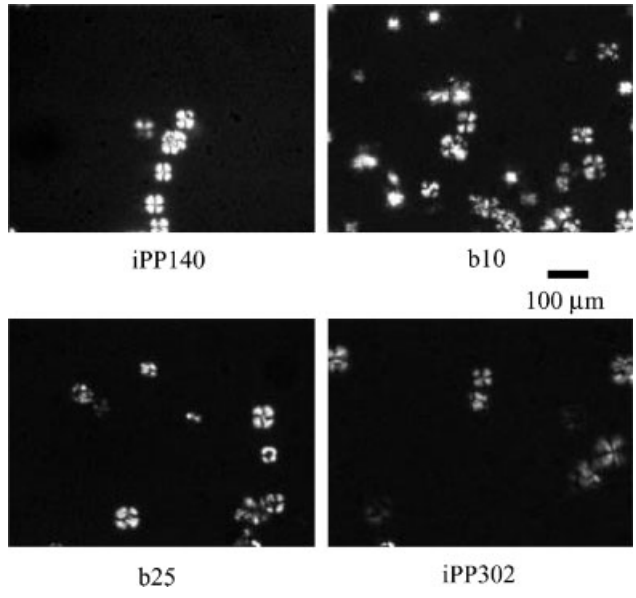

Figure 11. Optical micrographs of iPP samples after quiescent crystallization at 145 °C.

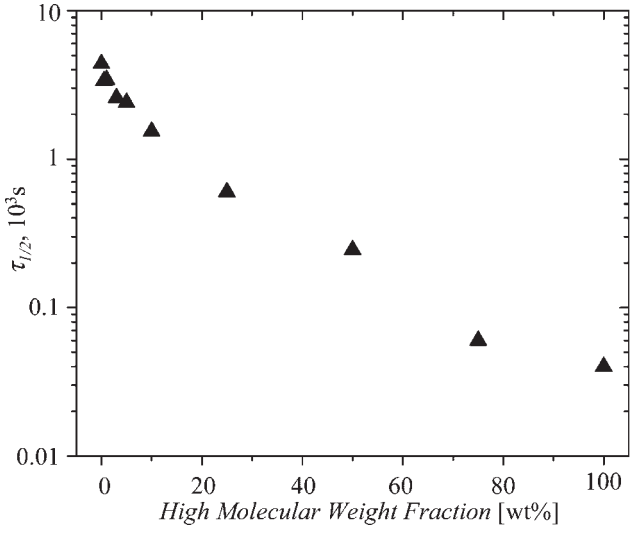

Figure 10. Crystallization of pre-sheared samples with increasing high molecular weight fraction. Characteristic crystallization half times at 145 °C.

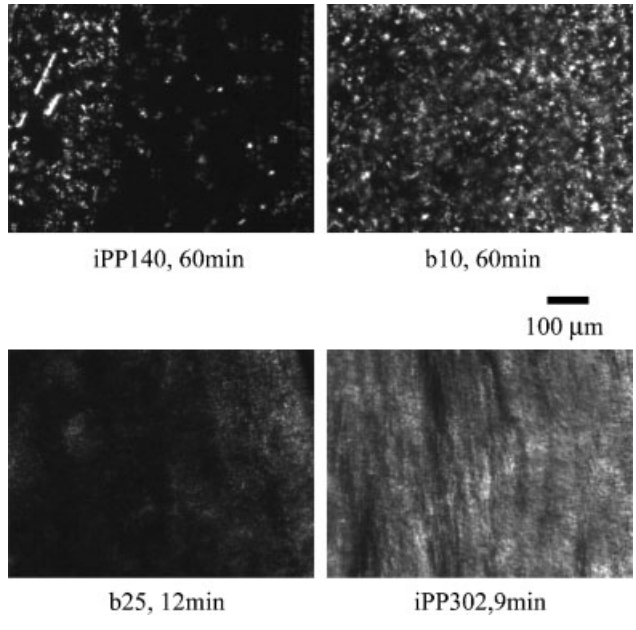

Figure 12. Optical micrographs of pre-sheared iPP samples at 145 °C. (Time represents instant at which snapshot was taken during experiment).

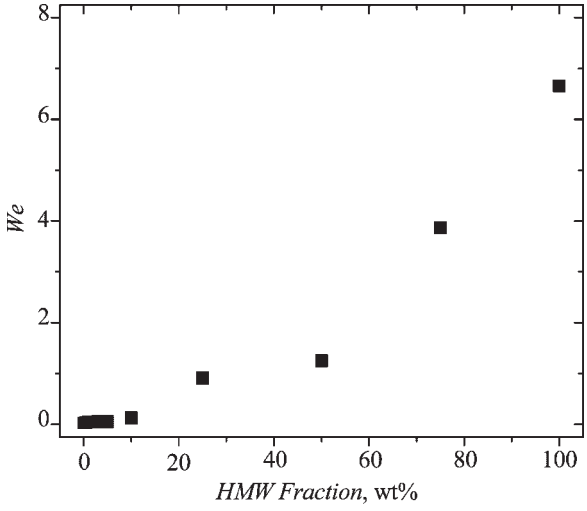

Figure 13. Weissenberg number as function of HMW fraction for sheared iPP blends.

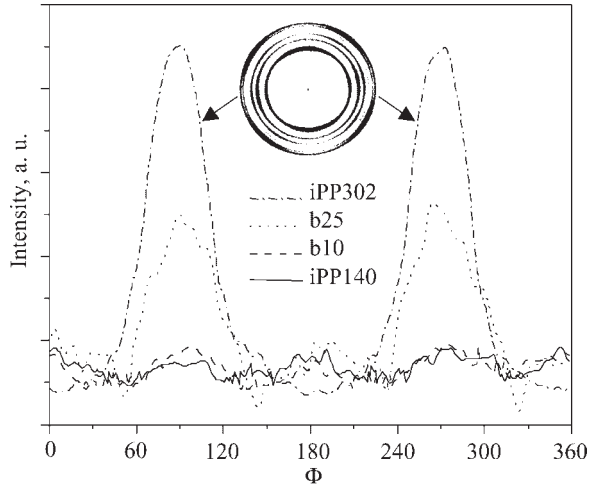

Figure 14. Azimuthal scan of the intensity of the 040 reflection (for α-crystals) or 113 reflection (for γ-crystals) from WAXD images of iPP pre-sheared samples. WAXD image of pre-sheared iPP302 is included in graph to demonstrate presence of γ-crystals (a weak ring on second position from the outside of the diffraction pattern).

number ($We = \dot{\gamma}\,\lambda_i$) at a value of about 1 (Figure 13).[14] For calculating *We* values, relaxation times, λ_i, were defined as the inverse of the crossover of G' and G'' frequency ω_i, as obtained from the master-curves shown in Figure 4 (see Table 2).

Wide Angle X-Ray Diffraction (WAXD)

The α and γ-crystalline forms of iPP have their own distinguishing reflections in their WAXD patterns.[19] Using an X-ray wavelength of 1.54 Å, the α-crystals are cataloged as follows: (110) at $2\theta = 14.1°$, (040) at 16.9°, (130) at 18.5°, (111) at 21.4°, and (−131) at 21.8°. The γ-crystals are indexed as follows: (111) at $2\theta = 13.8°$, (113) at 15.0°, (115) at 17.2°, (117) at 20.1°, (202) at 21.2°, and (026) at 21.9°. Most of the γ-crystals reflections are close and almost overlap with those of the α-crystals, however the (117) reflection of the γ-crystals is individually separated form all the reflections of the α-crystals. A (117) reflection generally indicates the presence of γ-crystals.

WAXD was performed on the cooled samples after completion of crystallization. For quiescently crystallized samples, the intensity of the WAXD reflections is uniform. Circular rings are observed, indicative of a random crystal orientation and only α-crystals are present in these samples.

WAXD patterns of pre-sheared samples start to become anisotropic for blends with HMW fractions of 25 wt.-% and higher. Figure 14 illustrates this anisotropy when azimuthally scanning the intensity of the 040 reflections. Samples iPP140 and up to 10 wt.-% HMW show isotropic reflections and α-crystals only. However, blend b25 and iPP302 show relatively narrow azimuthal breadths. Arcs in the equator are observed, indicative of a high crystalline orientation, and a reflection at $2\theta = 20.24°$ indicating the presence of γ-crystals in the samples.

Differential Scanning Calorimetry

DSC thermograms (heating rate of 5 $K \cdot min^{-1}$) of b10 after isothermal crystallization at 145 °C from three different experiments are compared in Figure 15. Quiescent crystallization was performed directly in the DSC. One sample was first quenched to room temperature before scanning and a second sample was scanned directly after crystallization. The third thermogram is of a pre-sheared sample recovered from the Linkam hotstage. The thermograms clearly show two peaks, one at about 156 °C attributed to crystals arising from the rapid quenching after isothermal crystallization, and a second peak at about 168 °C attributed to crystals formed during the isothermal crystallization.

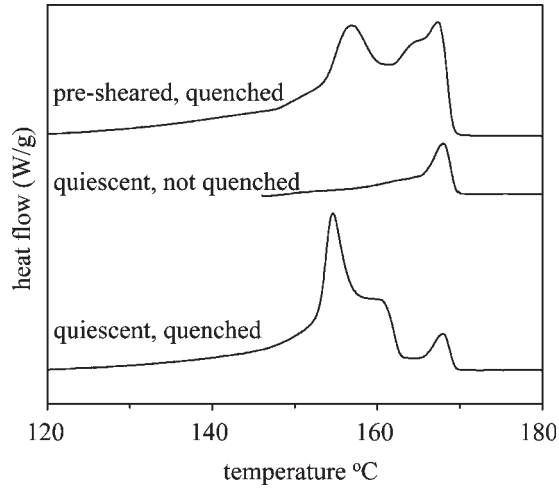

Figure 15. DSC thermograms at 5 $K \cdot min^{-1}$ of three iPP samples: one quiescently crystallized then quenched, a second quiescently crystallized and a third pre-sheared then quenched.

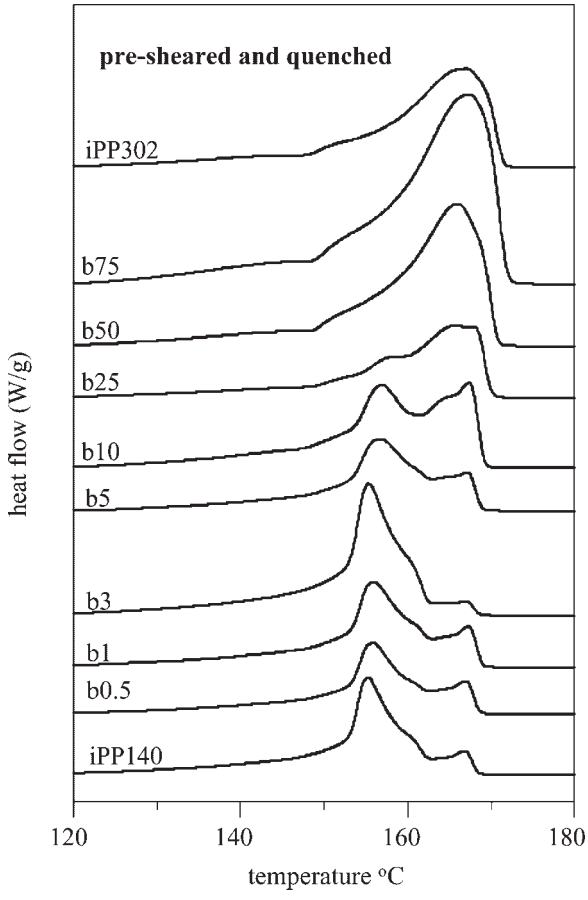

Figure 16. DSC thermograms of pre-sheared iPP samples after crystallization at 145 °C.

All the thermograms of the pre-sheared samples (Figure 16) show two major peaks. One peak at about 156 °C is attributed to crystals arising from the rapid quenching after isothermal crystallization; however, in this case this peak area decreases as the HMW fraction increases and almost vanishes in the iPP302 thermogram. This is expected since an increase in HMW fraction enhances the crystallization kinetics extensively and most of the sample is crystallized by the time the temperature is quenched to room temperature. The second peak, in this case at about 168 °C, is due to crystals formed during isothermal crystallization after application of a pre-shear. The area under the DSC curves increases as the amount of the long chains is increased.

Discussion

The dynamic moduli curves $G'(\omega)$ and $G''(\omega)$ of the iPP samples shift to lower frequencies when the HMW fraction is added. Surprisingly, they retain their shape to a degree that facilitates time-concentration shifting (as shown in Figure 5). The two polymers are fairly narrow in their molecular weight distribution but not narrow enough to exhibit the distinct bimodal mode distribution of binary blends.[20,21] The relaxation processes of the two polymers are too broadly distributed to be distinguished individually when blending the two polymers. $\lambda_{iPP302}/\lambda_{iPP140}$ is about 232 (see Table 2), which corresponds to an $\overline{M}_w$ ratio of about 5.3. This value is higher than the ratio obtained by GPC measurements of about 2. This inconsistency may be due to difficulties dissolving the polymer before the GPC analysis.

The experimental conditions for the crystallization study were intended to segregate the effects of undercooling and flow on the crystallization process of the iPP samples. Isothermal conditions, before flow application, are approached with the maximum cooling rate available while minimizing undercooling. The experimental temperature was selected close to the samples melting temperature. This low undercooling results in a low nucleation density and slow crystallization kinetics as necessary for ease of in situ optical and rheological observations. We chose identical shearing conditions for all samples (constant shear strain of 600 with a shear rate of 10 s^{-1} for a duration of 60 s) to specifically highlight the role of addition of one polymer to the other under similar temperature and deformation histories. The shear rate range is bounded by Linkam's experimental limits and because of the wide difference in pure polymer viscosities ($\eta_{iPP302}/\eta_{iPP140} \approx 250$ at $T_x =$ 145 °C), a value of applied shear rate was chosen suitable for all samples. Both homopolymers possess relaxation times that are far apart ($\lambda_{iPP302}/\lambda_{iPP140} = 232$ at $T_x = 145$ °C, see Table 2). Because of this, the use of the same shear rate on the samples resulted in increasing Weissenberg numbers with increasing HMW fraction (see Figure 13). A study on strain effects while keeping a constant Weissenberg number value is currently underway.

Addition of a second polymer with different molecular weight alters the crystallization kinetics significantly, as demonstrated by a change in characteristic crystallization half time; even though both homopolymers show virtually the same stereoregularity and the blends are homogenized following a most effective solution mixing procedure. For quiescent crystallization (Figure 8), it is interesting to note that (1) the crystallization rate is about the same for both pure LMW and HMW polymers and (2) addition of a small amount of a second polymer increases the nucleation rate. Surprisingly, the quiescent crystallization is accelerated in both cases, whether we add small amounts of HMW to LMW or the other way around. This is attributed to an increased nucleation density (increase by a factor of about 5, estimated from optical microscopy of Figure 11) which may be caused by composition fluctuations that may act as nuclei for starting crystal growth. Smith[22] has reported such fluctuations that led to fractionation in polyethylene binary systems during their solidification process when subjected to cooling rates lower than 20 $K \cdot min^{-1}$.

Long molecules greatly impact the crystallization behavior under flow conditions. Elongated structures (strings) appear in optical microscopy (see Figure 12). It is assumed that these are shish-kebab structures that grow during shear experiments in samples having 25 wt.-% or more in HMW fraction. Molecules are getting oriented in the flow direction as corroborated by arc appearances in the WAXD images (see Figure 14) of blends with 25 wt.-% and higher concentration HMW, thus giving rise to row nuclei upon shear application. These row nuclei then are assumed to lead to shish-kebab structure growth.

Long chains in blends with less that 25 wt.-% HMW fraction subjected to shear relax back to their random coil conformation after extension in the flow direction and give rise to spherulitic structures. Most of these composition levels are higher than the overlap concentration of the HMW sample iPP302, which is about $c^* = 0.8$ wt.-% (estimated using the Mark-Houwink-Sakurada equation,[23] to be 8.8×10^{-3} g $\cdot$ cm^{-3}; and converted to wt.-% using a density of 0.9 g $\cdot$ cm^{-3}). This implies that the blends have some degree of entanglement and that the shear applied on the overlapped (or somewhat entangled) polymer chains orient them in the flow direction but the chains then relax, crystallize in the form of lamellae and give a spherulitic structure. In a recent report Seki et al.[6] have shown that a concentration of HMW about the overlap concentration c^* was enough to produce shish-kebab structures and maximize the crystallization rate. However, in the presented results an increase in the crystallization rate beyond c^* and shish-kebab formation at fractions 30 times higher than c^* and above is shown.

Correlating the flow effects, using a Weissenberg number value of about $We = 1$ as a criterion for spherulitic to shish-kebab morphology transition,[14] with the addition of HMW fraction (see Figure 13) draws similar conclusions to results from OM and WAXD. Under the given experimental conditions, low HMW fraction samples (under 25 wt.-%) have *We* values below 1 while 25 wt.-% and higher HMW fraction samples have substantially higher *We* values since they possess larger relaxation times (the shear rate applied on all samples is constant). It needs to be mentioned that application of a higher shear rate, keeping the same shearing time in the above experiments, can shift this morphological transition to lower HMW fractions.

Conclusion

In a bimodally distributed polymer, addition of small amounts of the second component (same polymer but different molecular weight) can increase the nucleation density significantly. This expresses itself in a reduced crystallization time. The effect is not symmetric. Addition of small amounts of HMW (into LMW) reduces the crystallization time more dramatically than addition of small amounts of LMW (into HMW). The shortest crystallization time (at the given undercooling temperature) was found with about 10 wt.-% HMW in 90 wt.-% LMW.

Application of shear prior to isothermal crystallization also increases the nucleation rate. This effect is strongly enhanced when adding increasing amounts of HMW. Small amounts of HMW (overlap concentration for instance) have a large effect already. But the HMW sample crystallizes by far the fastest. The crystal morphology is also affected. Shish-kebab morphology (from optical micrographs) and γ-phase crystalline structure (from WAXD) appear after addition of about 25 wt.-% or higher of the HMW component in the LMW matrix. At this HMW composition level and higher, and within the experimental conditions applied, the Weissenberg number correlation at a value about $We = 1$ for spherulite to shish-kebab transition is supported.

Acknowledgements: The authors express their gratitude to the NSF-supported Materials and Research Science and Engineering Center on Polymer at UMass Amherst (DMR-0213695) for financial support and to Helmut Strey for the access to the X-ray facilities.

[1] A. J. Pennings, A. M. Kiel, *Kolloid Z. Z. Polym.* **1965**, *205*, 160.
[2] A. Keller, H. W. Kolnaar, ''Flow induced orientation and structure formation'', in: *Materials Science and Technology, Vol. 18: Processing of Polymers*, H. E. H. Meijer, Ed., Wiley-VCH, Weinheim 1997, p. 189.
[3] P. Jerschow, H. Janeschitz-Kriegl, *Int. Polym. Proc.* **1997**, *12*, 72.
[4] N. V. Pogodina, V. P. Lavrenko, S. Srinivas, H. H. Winter, *Polymer* **2001**, *42*, 9031.
[5] A. Nogales, B. S. Hsiao, R. H. Somani, S. Srinivas, A. H. Tsou, F. J. Balta-Calleja, T. A. Ezquerra, *Polymer* **2001**, *42*, 5247.
[6] M. Seki, D. W. Thurman, J. P. Oberhauser, J. A. Kornfield, *Macromolecules* **2002**, *35*, 2583.
[7] A. J. Pennings, J. M. A. A. Van der Mark, H. C. Booij, *Kolloid Z. Z. Polym.* **1970**, *236*, 99.
[8] A. J. Pennings, A. Zwijnenburg, K. E. Meihuizen, *Chim. Ind. (Milan, Italy)* **1977**, *59*, 729.
[9] G. Eder, H. Janeschitz-Kriegl, G. Krobath, *Prog. Colloid Polym. Sci.* **1989**, *80*, 1.
[10] H. Janeschitz-Kriegl, G. Eder, *J. Macromol. Sci. Chem.* **1990**, *A27*, 1733.
[11] S. Liedauer, G. Eder, H. Janeschitz-Kriegl, P. Jerschow, W. Geymayer, E. Ingolic, *Int. Polym. Process.* **1993**, *8*, 236.
[12] G. Kumaraswamy, A. M. Issaian, J. A. Kornfield, *Macromolecules* **1999**, *32*, 7537.
[13] R. H. Somani, L. Yang, I. Sics, B. S. Hsiao, N. V. Pogodina, H. H. Winter, P. Agarwal, H. Fruitwala, A. Tsou, *Macromol. Sympos.* **2002**, *185*, 105.
[14] A. Elmoumni, H. H. Winter, A. J. Waddon, H. Fruitwala, *Macromolecules* **2003**, *36*, 6453.

[15] S. Acierno, B. Palomba, H. H. Winter, N. Grizzuti, *Rheol. Acta* **2003**, *42*, 243.
[16] J. Xu, M. Johnson, G. L. Wilkes, *Polymer* **2004**, *45*, 5327.
[17] R. A. Gonzalez-Ruiz, R. L. Laurence, E. B. Coughlin, manuscript in preparation.
[18] S. Mori, H. G. Barth, ''*Size Exclusion Chromatography*'', Springer, Berlin 1999.
[19] B. Lotz, J. C. Wittmann, *Polymer* **1996**, *37*, 4979.
[20] H. Watanabe, T. Kotaka, *Macromolecules* **1984**, *17*, 2316.
[21] H. Knoglinger, A. Schausberger, H. Janeschitz-Kriegl, *Rheol. Acta* **1987**, *26*, 460.
[22] P. Smith, R. S. J. Manley, *Macromolecules* **1979**, *12*, 483.
[23] M. Kurata, Y. Tsunashima, M. Iwama, K. Kamada, ''Viscosity – Molecular Weight Relationships and Unperturbed Dimensions of Linear Chain Molecules'' in: *Polymer Handbook*, 2nd edition, J. Brandrup, E. H. Immergut, Eds., J. Wiley & Sons, New York 1975, p. IV–7.

